

Weak localization, fluctuation, and superconductivity in thin Nb films and wires

Makoto Hikita, Yukimichi Tajima, and Toshiaki Tamamura

Nippon Telegraph and Telephone Corporation, Opto-Electronics Laboratories, Tokai, Ibaraki 319-11, Japan

Susumu Kurihara

Nippon Telegraph and Telephone Corporation, Basic Research Laboratories, Musashino, Tokyo 180, Japan

(Received 27 December 1989; revised manuscript received 12 March 1990)

Weak localization, fluctuation conductivity, and related problems have been investigated based on a comprehensive set of experiments on transition metal Nb films and wires. The temperature dependence of the inelastic scattering rate $1/\tau_\phi$ of films with various thicknesses (25–80 Å), estimated from magnetoresistance data above T_c , is well fitted to a function of $C_0 + C_1T + C_3T^3$. The coefficient C_1 is in excellent quantitative agreement with the theoretical prediction of the electron-electron scattering mechanism for two-dimensional dirty metals. The coefficient C_3 shows no thickness dependence and is in semiquantitative agreement with theories of three-dimensional electron-phonon scattering mechanisms. The upper critical field of thin Nb wires with a width of less than 1000 Å exhibits unconventional temperature dependence close to T_c . We also discuss this behavior.

I. INTRODUCTION

Recently weak-localization theory and the electron-electron interaction theory have been used successfully to explain the anomalous magnetoresistance of superconducting disordered metals like Al films^{1–6} as well as that of thin normal metals like Mg, Cu, Ag, and Au films,⁷ by considering fluctuation conductivity effects. Furthermore, extensions of the interaction-effect theories⁸ have also been used to interpret experiments on T_c reduction^{9,10} and the effects on upper critical field H_{c2} (Ref. 4) in dirty superconducting thin films. One of the next main areas of interest is the possibilities of further progress to apply these predictions fully to transition metals with a higher T_c . Indeed, experiments have sometimes produced different results for the temperature dependence of the inelastic scattering rates $1/\tau_\phi$, for example, those of transition superconducting metals like Nb.^{3,11,12} On the other hand, the theory for T_c change in quasi-one-dimensional metals based on electron-electron interaction effects¹³ are insufficient to explain recent experiments on $\text{Mo}_{0.8}\text{Ge}_{0.2}$ thin film wires,¹⁴ although the experimental results on narrow Al films above T_c have been verified by the theoretical proposals on quasi-one-dimensional superconducting wires.¹⁵

In this paper, we report on a comprehensive set of studies on inelastic scattering mechanisms and superconducting parameters in thin and uniform Nb films with thickness from 25 to 80 Å, and provide a quantitative evaluation based on recent quantum transport theories. All films satisfy the characteristic length conditions in two dimensions (2D) for inelastic scattering, electron-electron scattering, and superconducting coherence lengths, and in three dimensions (3D) for the elastic scattering process. Since these assumptions frequently appear in theoretical calculations, they are appropriate for testing the predictions. We present a systematic

change of temperature dependence of $1/\tau_\phi$ in each film, and discuss this behavior compared with previous data. Additionally, T_c reduction of the films is also discussed, considering both size and bulk effects, namely 2D and 3D effects. On the other hand, the unusual behavior of temperature-dependent H_{c2} is found in Nb wires with a width of less than 1000 Å. The H_{c2} suddenly decreases when the temperature approaches T_c , while the film exhibits dH_{c2}/dT linear dependence like conventional dirty superconductors in the same temperature range. This size effect is thought to provide suggestive information with regard to recent experiments on $\text{Mo}_{0.8}\text{Ge}_{0.2}$ thin wires¹⁴ and is discussed phenomenologically based on the simple Ginzburg-Landau (GL) relation rather than on the interaction effects.

II. ANALYTICAL METHOD

A. Calculation of τ_ϕ

The temperature-dependent inelastic scattering time, τ_ϕ was calculated from the following formula considering weak localization (WL), Maki-Thompson fluctuation (MT), and Aslamazov-Larkin (AL) fluctuation for 2D.

$$\Delta(G)(H, T) = \Delta G_{\text{WL}}(H, T) + \Delta G_{\text{MT}}(H, T) + \Delta G_{\text{AL}}(H, T), \quad (1)$$

where $\Delta G(H, T) = G(H, T) - G(0, T)$ and $G(=1/R_\square, R_\square$: sheet resistance) is measured conductance at a fixed temperature. Each contribution is as follows.

For weak localization,¹⁶

$$\Delta G_{\text{WL}}(H, T) = G_{00} \left[\frac{3}{2} F(a_1) - \frac{1}{2} F(a_2) \right], \quad (2)$$

where $F(x) = \Psi(\frac{1}{2} + x) - \ln(x)$, Ψ is the digamma function, $a_1 = (H_\phi + \frac{4}{3}H_{s0})/H$, $a_2 = H_\phi/H$, $G_{00} = e^2/2\pi^2\hbar$

$= 1.235 \times 10^{-5} \Omega^{-1}$, H is an applied field, $H_x [= \Phi_0 / (4\pi D \tau_x)]$ is a corresponding field defined by x , τ_{so} is spin-orbit scattering time, $\Phi_0 = hc/2e = 2.07 \times 10^{-7} \text{ G cm}^2$, $D (= \frac{1}{3} v_F l)$ is the diffusion constant, l is the electron mean free path, and v_F is the Fermi velocity. In this estimation, the H_ϕ of Nb film is not sensitive to the value of H_{so} , then $H_{so} [\tau_{so} = 8 \times 10^{-13} \text{ sec (Ref. 17)}]$ is assumed to be constant. Actually, the magnetoresistance of the Nb film is positive, i.e., $H_{so} \gg H_\phi$.

For the Maki-Thompson fluctuation,¹⁸ when $\hbar/\tau_\phi \ll k_B T \ln(T/T_c)$ and $H \ll (ck_B T/4eD) \ln(T/T_c)$,

$$\Delta G_{MT}(H, T) = -\beta \Delta G_{WL}(H; H_{so} = 0, T), \quad (3)$$

where β is a function introduced by Larkin.¹⁸ In this study, the field-independent values of β are calculated at low-frequency from Eq. (8) in Ref. 18, and the restriction for $\hbar/\tau_\phi \ll k_B T \ln(T/T_c)$ is sufficiently satisfied. The restriction for H will be discussed in Sec. IV A.

For the Aslamazov-Larkin fluctuation,¹⁹

$$\Delta G_{AL}(T, H) = \frac{\pi^2}{4} G_{00} \frac{1}{\ln t} \left\{ 2x^2 \left[\Psi \left(\frac{1}{2} + \frac{x}{2} \right) - \Psi \left(1 + \frac{x}{2} \right) + \frac{1}{x} \right] - 1 \right\}, \quad (4)$$

where $x = H_c^*/H$, $H_c^* = \Phi_0/2\pi \xi^2(t)$, $\xi^2(t) = \xi^2(0)/\ln t$, $t = T/T_c$, $\xi^2(0) = 0.72 \xi_0 l$, $\xi_0 (= 0.18 \hbar v_F / k_B T_c)$ is the BCS coherence length, and k_B is the Boltzmann's constant.

As all measured films show superconductivity, the diffusion constant D is estimated from dH_{c2}/dT values. In this study, the D of each film is treated as 3D because the relation of $l < d$ is satisfied in all films, where d is the film thickness.

B. Inelastic scattering mechanisms

Temperature-dependent inelastic scattering time is mainly attributed to the electron-electron scattering time τ_{e-e} and the electron-phonon scattering time τ_{e-ph} .

Alt'shuler, Aronov, and Khmelnitsky²⁰ predict τ_{e-e} in 2D as

$$\frac{1}{\tau_{e-e}} = \frac{k_B T e^2}{2\pi \hbar^2} R_\square \ln \left[\frac{\pi \hbar}{e^2 R_\square} \right] = C_{1th} T. \quad (5)$$

The characteristic length scale for electron-electron scattering corresponds to the thermal diffusion length as $l_{th} = (\hbar D / k_B T)^{1/2}$; $l_{th} > d$ for 2D.

On the other hand, Abrahams *et al.*,²¹ and Fukuyama and Abrahams²² have calculated τ_{e-e} in 2D as the relation $1/\tau_{e-e} = C T \ln(T_1/T)$, where the details of constant values C and T_1 are described in Refs. 21 and 22. Recently Fukuyama²³ and Abrahams²⁴ have pointed out that the two equations arise from the same physical process. In this study, Eq. (5) is adopted for the evaluation of Nb films. It should be noted that the coefficient C_{1th} of Eq. (5) includes only one measuring parameter of R_\square .

Only electron-phonon scattering in pure metals has been studied in detail. In the clean 3D limit, when $q_T l > 1$, τ_{e-ph} is given by Lawrence and Meador²⁵ as

$$\frac{1}{\tau_{e-ph}} = 14\pi \zeta(3) \lambda \omega_D \left[\frac{T}{\Theta_D} \right]^3, \quad (6)$$

where q_T is the phone wave vector, $\zeta(x)$ is the Riemann's ζ function, λ is the electron-phonon coupling constant, ω_D is the Debye frequency, and Θ_D is the Debye temperature. In contrast, the theoretical calculation for τ_{e-ph} in dirty metals has been less developed. Schmid²⁶ predicts T^4 dependence of $1/\tau_{e-ph}$ for dirty 3D metals. A scattering rate of $1/\tau_{e-ph}$ proportional to T^2 is proposed by Takayama²⁷ and by Kagan and Zhernov.²⁸ As for the dirty 2D limit, the T^3 variation for $1/\tau_{e-ph}$ is derived from the expression for the clean 2D limit proposed by Raffy *et al.*²⁹ as

$$\frac{1}{\tau_{e-ph}} = 14\pi^2 \zeta(2) \frac{\lambda k_B l T^3}{\hbar d \Theta_D^2}. \quad (7)$$

This expression shows a similar temperature dependence to that in the clean 3D metals. Thus, the temperature dependence of τ_{e-ph} in dirty metals is complicated as described above.

Other important mechanisms of the inelastic scattering time are ascribed to spin-orbit scattering and magnetic impurity scattering. In the present experiment, both contributions are small and are assumed as temperature-independent constant values.

C. Electron interaction effect on T_c

Considering the electron interaction effect, the reduction of T_c in thin films with increasing disorder has been proposed in the weak localization regime by Ebisawa, Fukuyama, and Maekawa³⁰ as

$$\ln \left[\frac{T_c}{T_{c0}} \right] = -G_{00} R_\square g_1 N(0) \times \left\{ \frac{1}{2} \left[\ln \left[\frac{AT_c}{T_{c0}} \right] \right]^2 + \frac{1}{3} \left[\ln \left[\frac{AT_c}{T_{c0}} \right] \right]^3 \right\}, \quad (8)$$

where T_{c0} is the T_c of the pure limit, $R_\square (= \rho/d)$ is surface resistance, $g_1 N(0)$ is the coupling constant, and $A = 5.5 \xi_0 / l$. Equation (8) assumes that $l_{th} > d > l$, $\tau > \omega_D$, and $D(2\pi/d)^2 < 4\pi e \gamma \omega_D$, i.e., the system is 2D for the electron interaction and 3D for the elastic scattering. Consequently T_c linearly decreases with film thickness when ρ is constant.

III. EXPERIMENTAL PROCEDURE

A. Film preparation

Because Nb has a strong affinity to oxygen, the Nb oxide is grown along grain boundaries. The existence of a native oxide makes it difficult to determine the film thickness of the metallic part and increases the inhomogeneity

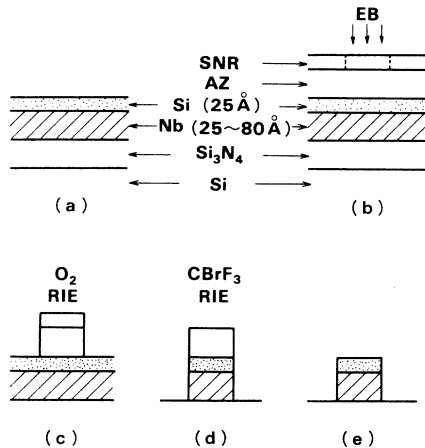


FIG. 1. The preparation process of films (a) and wires (b)–(e) are schematically described.

of the film. Thus it is important to suppress the growth of Nb oxide on the surface as much as possible, in order to prepare continuous and uniform Nb thin films.

The Nb film preparation method is schematically shown in Fig. 1(a) and is described below. 2000-Å-thick Si₃N₄ films, prepared by chemical vapor deposition on a Si wafer, were used as substrates to avoid interface oxidation between the Nb film and the substrate. After the Si₃N₄ surface had been sputtered by Ar ions to remove surface contaminations, Nb films were successively deposited on the substrate by the electron beam evaporation method using a 99.99% Nb pellet under a pressure of $(1-4) \times 10^{-7}$ Torr at room temperature. The Nb film thicknesses of 25, 30, 40, 50, 60, and 80 Å were determined using a crystal thickness monitor of an almost constant deposition rate of 1 Å/sec. Thin Si film of 25 Å was continuously deposited on the Nb surface to protect it from the atmosphere. By these procedures, the oxidation of very thin Nb films can be almost completely avoided.³¹ This was confirmed by resistivity measurements.

B. Wire preparation

The process for fabricating thin Nb wires is also shown in Fig. 1. The wires were patterned by the electron beam (EB) process using the two-layer resist system of a silicone-based negative resist [(SNR)/AZ-type photoresist and by reactive ion etching (RIE)].³² Firstly, AZ resist was coated on the substrate to a thickness of about 2000 Å. It was then baked at a low temperature of 120 °C to permit the use of a wet process (methyl-ethyl-ketone) for the final removal of the AZ resist. The SNR was coated on the AZ resist, was patterned by finely focused EB exposure (Elionix: ELS-5000), and was developed. The SNR patterns were transferred to the AZ layer by O₂ RIE. Four-terminal Nb patterns were etched using CBrF₃ RIE.

To achieve the fine Nb patterning, the choice of the RIE etching table is very important. When an SiO₂ table

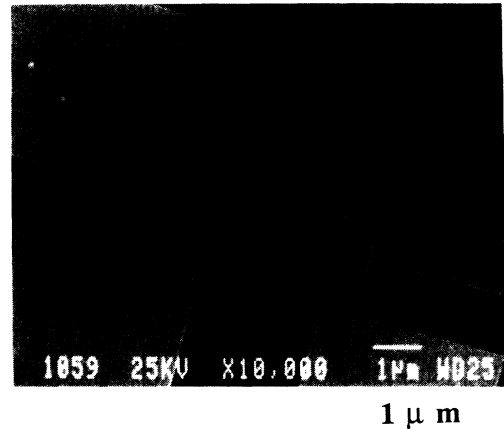


FIG. 2. SEM photograph of Nb patterns with 1000-Å-width and 80-Å-thickness Nb pattern used for the measurement.

was used, sufficient side etching was observed. In contrast, when a carbon table was used, islandlike remnants appeared. However, no side etching and no remnant was observed when a combined SiO₂-carbon table was used.

Figure 2 shows the four-terminal Nb pattern 1000-Å wide and 80-Å thick used for the measurements. This was obtained by using CBrF₃ RIE and the SiO₂-carbon table under a pressure of 3 Pa and at a power of 0.18 W/cm². Finally, all the films and wires were coated with thin AZ resist to protect them from the atmosphere during measurement.

It should be noted that native oxide growth on the wire sidewalls was unavoidable in the process. Since the sidewall oxide thickness was impossible to determine directly, it was assumed to be equal to the surface oxide thickness which was exposed to the atmosphere. The surface oxide thickness of the Nb films was determined as approximately 50 Å using x-ray photoelectron spectroscopy (XPS). Our results agree with those of Grunder and Halbritter.³³

C. MEASUREMENTS

The T_c , H_{c2} , and magnetoconductance were measured by the four-terminal ac (73 Hz) method and the four-terminal ac (73 Hz) bridge method which consisted of two highly sensitive lock-in amplifiers (PAR5301). To avoid the heating effect, the flowing current was controlled in 50–500 nA for films and 1–20 nA for wires. A magnetic field generated by a superconducting magnet (5 T: Vacuum Metallurgical Co. Ltd., 8T: Oxford Instrument Co.) was applied perpendicular to the Nb surface, while the current flowed perpendicular to the applied magnetic field. The temperature was determined with a calibrated carbon-glass thermometer (Lake Shore Cryotronics, Inc.)

IV. RESULTS AND DISCUSSION

A. Inelastic scattering mechanisms for thin films

The measured and calculated values of magnetoresistance $\Delta R [= R_{\square}(H, T) - R_{\square}(0, T)]$ are shown in Fig. 3

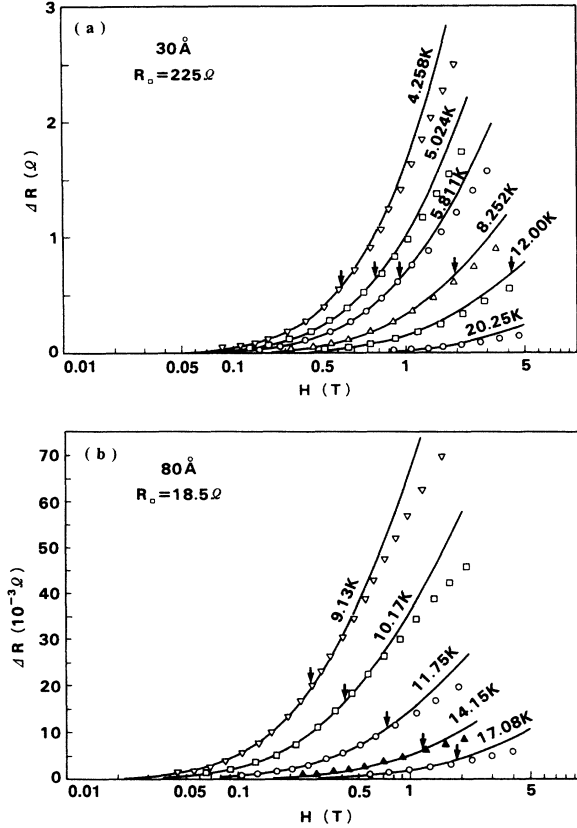


FIG. 3. The applied field dependence of magnetoresistance in (a) 30-Å and (b) 80-Å Nb films at various temperatures. Solid lines are best fitted curves for estimating τ_ϕ . Arrows indicates $H^* [= (ck_B T / 4De) \ln(T/T_c)]$ at each temperature.

for films with thicknesses of 30 and 80 Å. At each fixed temperature, the parameters of τ_ϕ are determined from the better fitting curves in the field below $H^* [= (ck_B T / 4De) \ln(T/T_c)]$, in order to satisfy the restrictions for the applied field H on the validity of Eq. (3). The τ_ϕ values for 25- and 50-Å films are also estimated by the same procedure. The temperature dependence of τ_ϕ is shown in Fig. 4. The τ_ϕ s appear to follow a relation of $T^{-\alpha}$ in the temperature range above 10 K where α changes monotonically from 1.6 to 3 as the film thickness is increased. However, these values are considerably better fit to the following equation

$$1/\tau_\phi = C_0 + C_1 T + C_3 T^3, \quad (9)$$

than to the power law of $T^{-\alpha}$ except in the temperature region close to T_c . A similar equation has been found for Al,^{2,6} Pd,²⁹ and Nb (Ref. 11) films. The C_0 , $C_1 T$, and $C_3 T^3$ terms in Eq. (9) correspond to magnetic-impurity, electron-electron, and electron-phonon inelastic scattering time, respectively.

The theoretical values of C_{1th} of all films are in excellent agreement with our C_1 data. This result reveals that Eq. (5) reflects the case an actual dirty metal. Additionally, this result clearly indicates that the dimensionality of the films satisfies the 3D conditions for an elastic scatter-

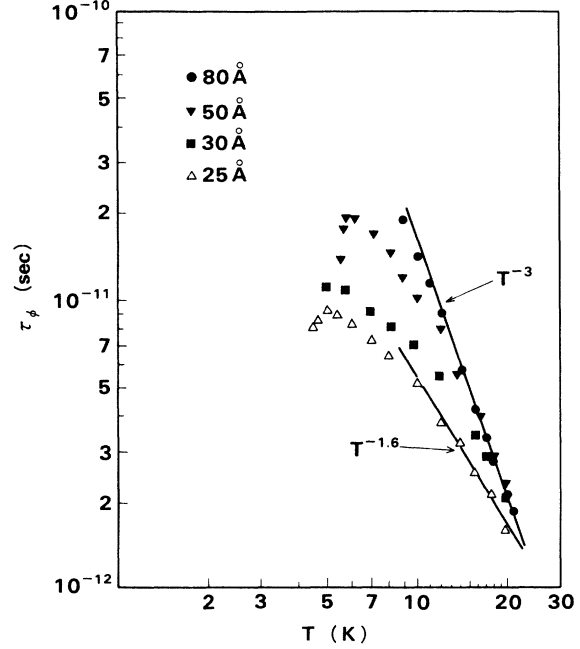


FIG. 4. The temperature dependence of τ_ϕ of various thickness films.

ing and the 2D conditions for an inelastic scattering, i.e., $l < d < l_{th}$. The obtained R_\square and other parameters are listed in Tables I and II.

The experimentally obtained values of C_3 are also listed in Table II. The T^3 dependence of τ_{e-ph} , is predicted for clean 3D films and dirty 2D films. Each was calculated using Eqs. (6) and (7), where the following values are used; $\Theta_D = 277$ K,³⁴ $\lambda = 0.9$.³⁵ If the phonon dimensionality reflects the dimensionality of τ_{e-ph} and a simple relation for transverse phonon wavelength λ_T is assumed, the Nb films in this experiment seem to be 2D except that with a thickness of 80 Å, which is in the crossover region from 3D to 2D. Because λ_T is estimated as 100 Å at 10 K, where $\lambda_T \times q_T = 2\pi$, $q_T = k_B T / \hbar v_s$, q_T is the phonon wave vector, and v_s is the speed of sound (2.2×10^5 cm/s).¹¹ However, the C_3 values are approximately constant for each film, i.e., they behave as in the 3D case, while the C_{3th} of Eq. (7) for 2D is highly dependent on film thickness. Bergmann pointed out⁵ that three dimensionality is enhanced in deposited films in contact with a substrate. According to the experimental study of Nb thin films by Park and Geballe,³⁵ the change of λ is believed to be less than 10% for all film thickness in the present experimental range. This suggests that the phonon mode is not drastically changed, i.e., there is no clear change of phonon dimensionality from 3D to 2D, although the small change of λ has a strong influence on T_c . Therefore, the electron-phonon scattering is believed to behave with 3D characteristics. Indeed, evident 2D behavior of electron-phonon scattering has not been reported experimentally for dirty, thin metal films.

It should be noted that τ_ϕ values in the vicinity of T_c decrease as the temperature is decreased in 25 and 50 Å thick films. This is qualitatively consistent with the

TABLE I. Measured and estimated parameters of Nb films. In this estimation, $v_F=2.73 \times 10^7$ cm/sec in Ref. 44, and other relations are described in the present paper.

| Thickness (Å) | 80 | 60 | 50 | 40 | 30 | 25 |
|--|------|-------|------|------|-------|------|
| Measured | | | | | | |
| T_c (K) | 7.51 | 6.71 | 5.45 | 4.71 | 2.78 | 2.13 |
| R_{\square} (at 10 K, Ω) | 18.5 | 30.9 | 62.1 | 98.2 | 225 | 330 |
| ρ (at 10 K, $\mu\Omega\text{cm}$) | 14.8 | 18.5 | 31.1 | 39.3 | 67.5 | 82.5 |
| dH_{c2}/dT (T/K) | 0.51 | 0.585 | 0.60 | 0.63 | 0.82 | 0.90 |
| Estimated | | | | | | |
| T_{c0} (K) | 7.75 | 7.5 | 6.7 | 6.2 | 4.7 | 4.0 |
| D (cm^2/sec) | 1.57 | 1.44 | 1.33 | 1.27 | 0.975 | 0.89 |
| l (Å) | 16.8 | 16 | 14.6 | 14 | 10.7 | 9.76 |
| ξ_0 (Å) | 484 | 500 | 560 | 605 | 799 | 938 |
| $\xi(0)$ (Å) | 90.1 | 89.4 | 90.4 | 92.0 | 92.5 | 95.7 |
| $D(2\pi/d)^2$ (10^{13} sec^{-1}) | 9.6 | 16 | 21 | 31 | 43 | 56 |
| $g_1 N(0)$ | | 4.7 | 3.7 | 2.8 | 1.7 | 1.2 |

strong effect of fluctuation in the region close to T_c (Ref. 2) although quantitative evaluation is difficult because the β function depends on an applied field.

The temperature dependence of τ_{ϕ} is compared with previous data. An early work on Nb films reported its relation to the power law of $T^{-\alpha}$.³ In this study, the contributions of τ_s , τ_{e-e} , and τ_{e-ph} to the τ_{ϕ} of the thinner films at 10 K are of the same order. Because of this, the temperature dependence of τ_{ϕ} appears to behave as a power law. This is thought to be one of the reasons for the various power-law values of temperature-dependent τ_{ϕ} in previous reports. Actually, this study reveals that the systematic variation of the temperature dependence of $T^{-\alpha}$ clearly divides each contribution between each temperature dependent factor. Dalrymple *et al.*¹¹ found the temperature dependence of Eq. (9) for τ_{e-ph} and τ_{e-e} , and reported that these values were in good agreement with the obtained theoretical values of Eqs. (5) and (6), respectively. Their results are essentially the same as ours except for those near T_c , where they as well as Gershenzon, Gubankov, and Zhuravlev³ did not observe the divergent behavior of τ_{ϕ} . However, our data shows this divergent behavior. This is thought to be attributable to the same origin as that in Al films in Ref. 2.

It is concluded that, in Nb films with R_{\square} in the range from 20–300 Ω , the inelastic mechanisms are 3D electron-phonon scattering and 2D electron-electron scattering and that the inverse of τ_{ϕ} increases divergently as it approaches T_c .

Figure 5 shows the temperature dependence of resis-

tance for 50-Å film under various magnetic fields. Since the resistance decreases with temperature under a low magnetic field below H_{c2} (estimated as 3 T) due to the effect of strong fluctuation conductivity, the temperature dependence of resistance is only discussed for a high magnetic field above H_{c2} in the temperature region below T_c . According to the interaction theory,³⁶ the lowest-order quantum corrections in the electron-electron interaction subdivide into the contributions of the particle-hole pair (g_1, g_3) and the particle-particle pair (g_2, g_4). In a high field ($H \gg ck_B T/4eD$ and $c\hbar/4eD\tau_{\phi}$), the temperature dependence of quantum effect contributions should be suppressed except for the particle-hole pair. It can be described as $\Delta G = G_{00}(g_1 - g_3)\ln T$ when $\tau_{so}, \tau_{\phi} \gg \tau_s$ and $\tau_{so}, \tau_s \gg \tau_{\phi}$, where ΔG is the quantum corrections. Assuming the screened Coulomb type of electron-electron interaction, $g_1 = 1$ and $g_3 = F/2$, where F is the degree of Coulomb screening; $F = 1$ for complete screening and $F = 0$ for bare interaction. Then the value of $(g_1 - g_3)$ should be equal to or less than unity according to the theoretical prediction. When the temperature dependence of quantum correction terms is described as $\Delta G = -G_{00}\alpha_g \ln T$, however, α_g exceeds unity with a value of 1.2 at 7 T and 1.8 at 6 T below 3 K in this experiment. Gershenzon, Gubankov, and Zhuravlev³ also found experimentally a similar relation where $\alpha_g = 1.2 - 1.6$ for Nb and Al films. Taking the excellent agreement between theory and experiment above T_c into account, this behavior is a little peculiar. We have no obvious explanation for this phenomenon at present.

TABLE II. Estimated and calculated values of C_0, C_1 , and C_3 .

| Thickness | 80 Å | 50 Å | 30 Å | 25 Å |
|--|-------------------|----------------------|----------------------|----------------------|
| C_0 (sec^{-1}) | 5.0×10^9 | 3.5×10^{10} | 6.5×10^{10} | 6.9×10^{10} |
| C_1 ($\text{K}^{-1} \text{sec}^{-1}$) | 9.1×10^8 | 1.15×10^9 | 4.0×10^9 | 6.8×10^9 |
| C_3 ($\text{K}^{-3} \text{sec}^{-1}$) | 5.7×10^7 | 4.8×10^7 | 4.0×10^7 | 5.6×10^7 |
| C_{1th} ($\text{K}^{-1} \text{sec}^{-1}$) | 6.1×10^8 | 1.7×10^9 | 4.6×10^9 | 6.1×10^9 |
| C_{3th} ($\text{K}^{-3} \text{sec}^{-1}$) (3D) | 9.1×10^7 | 9.1×10^7 | 9.1×10^7 | 9.1×10^7 |
| C_{3th} ($\text{K}^{-3} \text{sec}^{-1}$) (2D) | 8.1×10^7 | 11.3×10^7 | 13.8×10^7 | 15.1×10^7 |

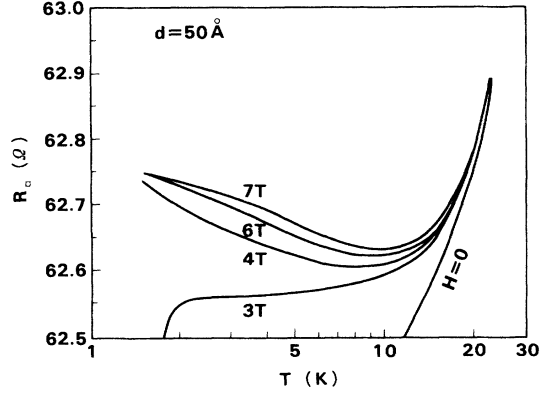


FIG. 5. The temperature dependence of resistance of the 50-Å-thick film in various fields.

B. T_c of thin Nb films

Figure 6 shows both the film thickness and the R_{\square} dependence of T_c in the Nb films. Recently Maekawa and Fukuyama³⁷ proposed a theory based on the Coulomb interaction effect in disordered systems stating that T_c decreases in proportion to R_{\square} in two-dimensional superconductors while ρ is constant. Subsequently this relation has been experimentally observed in relatively dirty superconductors such as *a*-WRe (Ref. 9) and *a*-MoGe (Ref. 10) films with $R_{\square} > 100 \Omega$. However, the T_c decrease of the Nb films is not proportional to R_{\square} as shown in Fig. 6. On the other hand, Camerlingo *et al.*³⁸

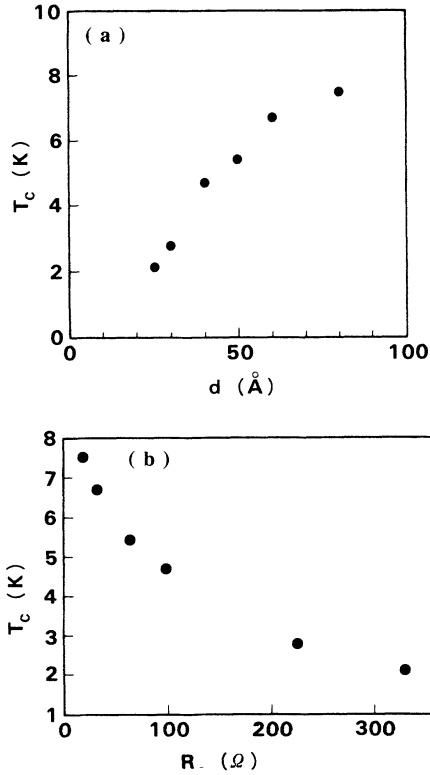


FIG. 6. (a) The film thickness and (b) R_{\square} dependence on T_c .

emphasize that for bulk 3D Nb films the lifetime broadening of the density of state has a much stronger influence on the T_c decrease than the interaction effects. Indeed, this behavior has been observed by some researchers.^{31,38,39} These results are all in good agreement as shown by the solid line in Fig. 7, where our data for thin films are also shown. In this study, ρ of Nb films increases as the thickness decreases as shown in Table I. The reduction of T_c in this study is more rapid than those previously reported for bulk samples. Additionally, as $l_{th} > d > l$ in this experiment, the dimensionality of the interaction effects is 2D. Therefore, it is believed that in the present experiment the T_c reduction confusedly reflects both 3D (bulk) and 2D effects.

Assuming that the origin of ΔT_c is only attributed to the interaction effects, $g_1 N(0)$ is calculated using Eq. (8), where ΔT_c is the discrepancy between bulk and film samples, i.e., $\Delta T_c = T_{c0} - T_c$. We imply that the proximity effect is negligible in this case as well as in that reported by Park and Geballe³¹ because no effective proximity layer exists in our films. The results are listed in Table I. The values of $g_1 N(0)$ increase with the thickness of the films. For the thinner films of 25 and 30 Å, the obtained values of approximately unity are roughly equal to those of extremely dirty metals such as *a*-WRe (Ref. 9) and *a*-MoGe.¹⁰ Equation (8) is derived for the case of $\tau^{-1} > \omega_D$ and $D(2\pi/d)^2 < 4\pi e^{\gamma} \omega_D$. These relations are satisfied by our films, where roughly estimated values are that $\tau^{-1} \sim 2 \times 10^{14}$, $\omega_D \sim 3.6 \times 10^{13}$, $D(2\pi/d)^2 \sim 10^{14}$, and

$$4\pi e^{\gamma} \omega_D \sim 6 \times 10^{14}.$$

On the other hand, according to the theoretical calculation considering the dynamically screened Coulomb interaction for the case of $\tau^{-1} < \omega_D$ (Ref. 40), the $g_1 N(0)$ in Eq. (8) is taken to be 4.9. The obtained value of 4.7 for the thicker films of 60 Å is equivalent to the theoretical value although the restriction of $\tau^{-1} < \omega_D$ is not satisfied

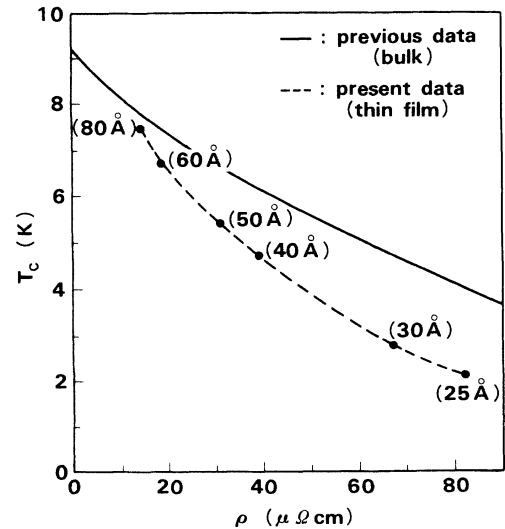


FIG. 7. The resistivity dependence of T_{c0} of bulk and T_c of thin-film Nb. The solid line describes the previous data (Refs. 31, 38, and 39) for T_{c0} of bulk Nb films.

even for the thicker Nb films. The $g_1 N(0)$ of 3.9 was also reported for the relatively clean Al films.⁴ Although a little ambiguity remains in the relation between τ^{-1} and ω_D , the values of $g_1 N(0)$ in this experiment are believed to be in the reasonable range estimated from the recent 2D interaction theories for disordered superconductors.^{30,40} The aforementioned results reveal that ΔT_c is essentially attributable to the interaction effects in thin metals.

C. Upper critical field H_{c2} and T_c in thin wires

The resistive T_c transition curves of three thin film wires with 80-Å thickness are shown in Fig. 8, where the widths of the wires are 4 μm , 1000 Å, and 500 Å. In these wires, neither sidewall is protected against the at-

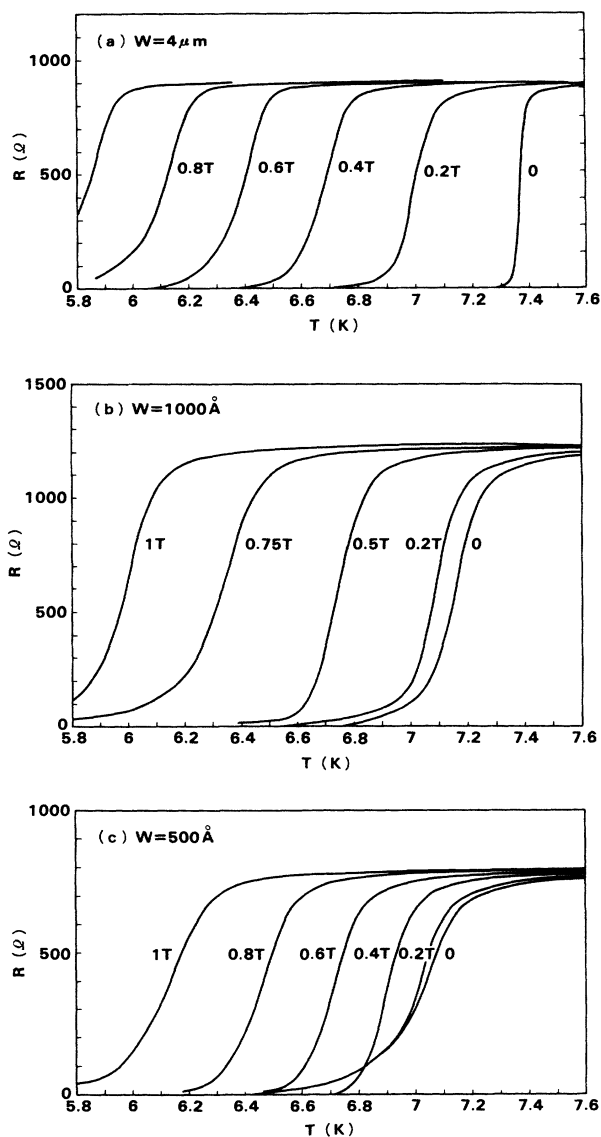


FIG. 8. The resistive T_c transition curves of thin-film wires with 80-Å thickness in various field; (a) 4- μm width, (b) 1000-Å width, and (c) 500-Å width.

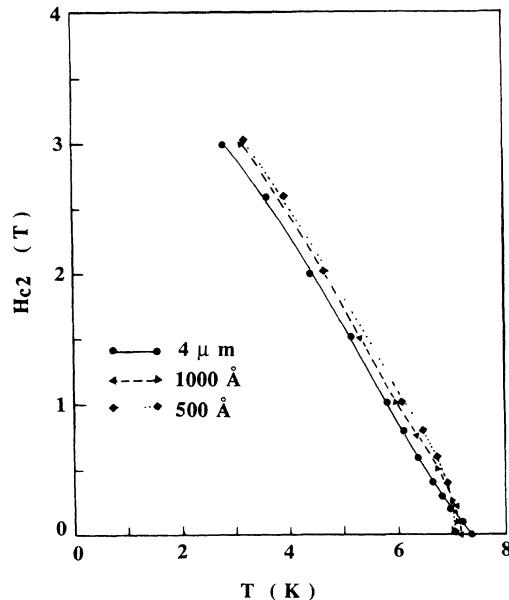


FIG. 9. The temperature dependence of H_{c2} of Nb wires.

mosphere. Figure 9 shows the temperature dependence of H_{c2} for each wire, where T_c is defined as the midpoint of the resistive transition curve. For the 4- μm -width wire, $H_{c2}(T)$ decreases linearly with temperature, although a slight upward curvature is observed which is regarded as a manifestation of the electron interaction effect proposed by Maekawa, Ebisawa, and Fukuyama.⁴⁰ In contrast, it is clearly observed that the $H_{c2}(T)$ curves of the 1000-Å and 500-Å wires near T_c deviate from a linear relation and follow the relation of $(T - T_c)^{-\gamma}$ where $\gamma = \frac{1}{2}$. This behavior is accompanied by T_c reduction and is not changed irrespective of the T_c definition point as shown in Fig. 8. First we checked the problem of the critical current of the wires. The results were the same in their experimental accuracy under both sets of experimental conditions at applied currents of 1 and 18 nA corresponding to 1.3×10^2 and 2.25×10^3 A/cm², respectively. Since the dH_{c2}/dT values are approximately equal for the three samples, it is believed that the conductive characteristics are free from the effects of etching damage. Therefore, it is concluded that the anomalous temperature dependence of H_{c2} near T_c is a size effect. However, it is not thought to be the dimensional crossover from 2D to 1D of the interaction effects of which the characteristic length l_{th} , estimated at less than 200 Å, is substantially shorter than the effective conducting wire width. Here the effective conducting width W_{eff} is defined as 100 Å less than that of its geometrical width, taking account of the oxide growth on both sidewalls after dry etching. Santhanam, Wind and Prober,⁶ have observed a similar H_{c2} curve phenomenon in Al wires and explained that it is attributable to the dimensional crossover of $\xi(t)$ from 2D to 1D near T_c . In our experiment, it should be noted that the deviation of $H_{c2}(t)$ from the linear relation seems to correspond, approximately, to the temperature at which $\xi(t) = W_{eff}/2$.

In seeking a qualitative explanation for the T_c reduction in narrow wires, a phenomenological approach is presented to deal with, very roughly, the size and fluctuation effects. Because the coherence length $\xi(t)$ near T_c is limited at the wire width, the order parameter fluctuation becomes stronger in the vicinity of T_c . This is believed to be one of the causes for the T_c reduction. The size effect reflects the assumption of $d\Psi/dx|_{x=\pm W/2}=0$ in Eq. (10). The order parameter in the wire is simply assumed $|\nabla\Psi|^2 \rightarrow |\Psi|^2 W^2$. The GL free energy, F_{GL} , in the absence of a field is given by

$$F_{GL} = \int d^3r (a|\Psi|^2 + \frac{1}{2}b|\Psi|^4 + c|\nabla\Psi|^2),$$

$$\left. \frac{d\Psi}{dx} \right|_{x=\pm W/2} = 0, \quad (10)$$

$$a = \alpha t_r, \quad b = \alpha/n_e, \quad c = \hbar^2/4m,$$

$$\alpha = \frac{6\pi^2}{7\zeta(3)} \frac{(k_B T_c)^2}{\varepsilon_F}, \quad t_r = \frac{T - T_c}{T_c}, \quad T_c = T_{c0}(W \rightarrow \infty),$$

where $\zeta(x)$ is the Riemann ζ function, W is the wire width, and the x axis is defined along the direction of W . When T is near T_c , the following approximate expres-

$$\frac{\langle |\Delta|^2 \rangle}{(k_B T_c)^2} = \frac{4\varepsilon_F}{3n_e k_B T_c} \left[t_r + \frac{7\zeta(3)}{8\pi^2} \frac{\langle |\Delta|^2 \rangle}{(k_B T_c)^2} + \frac{7\zeta(3)}{12\pi^2} \frac{\varepsilon_F \varepsilon_W}{(k_B T_c)^2} \right]^{-1},$$

where the energy $\varepsilon_W = \hbar^2/2mW^2$ characterizes the size effect that when T is not too close to T_c , the nonlinear fluctuation can be ignored. The T_c reduction caused by the size effect is obtained:

$$\Delta T_c = T_{c0} - T_c = -\frac{\delta T_c}{T_{c0}} = \frac{7\zeta(3)}{12\pi^2} \frac{\varepsilon_F \varepsilon_W}{(k_B T_c)^2}, \quad (13)$$

We find that the T_c reduction is proportional to ε_W , namely W^{-2} . When W is 500 Å, ΔT_c of 5–7 K is roughly estimated from Eq. (13). This value is an order of magnitude larger than those obtained from the experiment. Although our approximation here is very crude, the qualitative conclusion that $\Delta T_c \propto W^{-2}$ is believed to be of general validity. Indeed, a similar W^{-2} dependence of T_c reduction was also observed in Mo-Ge wires by Graybeal *et al.*¹⁴ Our result, however, is not sufficient for a quantitative explanation of the T_c reduction.

V. CONCLUSIONS

The primary objective of this work is to verify the quantum transport effects in thin Nb films and wires

sions are substituted for the last two terms on the right of Eq. (10) that

$$|\Psi|^4 \rightarrow \langle |\Psi|^2 \rangle |\Psi|^2 + |\Psi|^2 \langle |\Psi|^2 \rangle - (\langle |\Psi| \rangle)^2$$

and $|\nabla\Psi|^2 \rightarrow |\Psi|^2/W^2$, the latter being the result of the boundary conditions. In this crude approximation, the integral can be replaced by the multiplicative volume factor V . The GL free energy then takes a very simple form:

$$F_{GL} \sim F_{\text{eff}} = Va'|\Psi|^2, \quad a' = a + b\langle |\Psi|^2 \rangle + C/W^2. \quad (11)$$

In Eq. (11), the terms of $b\langle |\Psi|^2 \rangle + C/W^2$ corresponds to the renormalization of T_c . When the average of $\langle |\Psi|^2 \rangle$ is calculated using F_{eff} , we find the self-consistency equation of $\langle |\Psi|^2 \rangle$:

$$\langle |\Psi|^2 \rangle = \frac{\int d^2\Psi |\Psi|^2 e^{-\beta F_{\text{eff}}} / \int d^2\Psi e^{-\beta F_{\text{eff}}}}{BV(a + b\langle |\Psi|^2 \rangle + C/W^2)}. \quad (12)$$

Using the relation that

$$\langle |\Psi|^2 \rangle = \frac{7\zeta(3)}{8\pi^2} \frac{n_e}{(k_B T_c)^2} \langle |\Delta|^2 \rangle,$$

we have

based on recent theories on the weak localization and the electron-electron interaction effects. We have frequently found complicated behavior between the bulk and size effects which manifested themselves in the experimental results. This study proves that systematic change of the system size is effective in helping us understand how to disentangle each contribution.

For films, the τ_ϕ temperature dependence systematically changes with film thickness and is in good agreement with the theoretical predictions for 2D electron-electron scattering and 3D electron-phonon scattering. The reduction of T_c in thin films is explained by bulk and 2D effects.

For wires, we find anomalous H_{c2} behavior near T_c , accompanied by T_c reduction. A phenomenological explanation is attempted considering the finite wire width. A microscopic approach is also required for complete understanding.

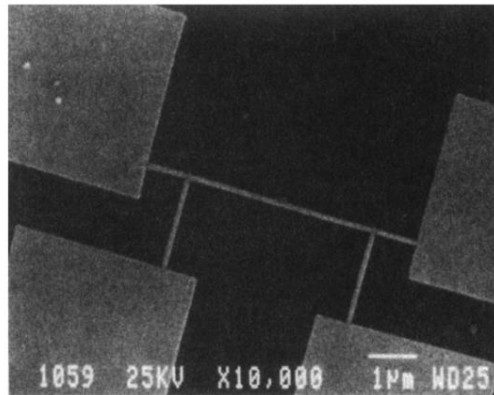
Very recently new terms of the MT- and the AL-Zeeman effects have been found for the fluctuation conductivity in high- T_c oxide superconductors.^{41–43} These effects are thought to be applicable to both conventional and high- T_c superconductors. The study of this problem has not been undertaken in previous studies for conventional superconductors. Further detailed investigations will be necessary to clarify this problem.

ACKNOWLEDGMENTS

The authors would like to thank K. Murase, T. Miyashita, H. Hiratsuka, and A. Yamaji for their support and encouragement throughout the study. The authors would also like to thank M. Kakuchi, A. Sugita, and O.

Niwa for discussions and for suggesting the microfabrication technique, M. Sekimoto for the Si_3N_4 preparation, M. Suzuki for the x-ray photoemission spectroscopy (XPS) analysis, M. Suzuki, K. Semba, N. Hatakenaka, and H. Nakano for helpful discussions.

- ¹Y. Bruynseraede, M. Gijs, C. Van Haesendonck, and G. Deutscher, *Phys. Rev. Lett.* **50**, 277 (1983).
- ²J. M. Gordon, C. J. Lobb, and M. Tinkham, *Phys. Rev. B* **28**, 4046 (1983); J. M. Gordon, C. J. Lobb, and M. Tinkham, *ibid.* **29**, 5232 (1984); J. M. Gordon and A. M. Goldman, *ibid.* **34**, 1500 (1986).
- ³G. E. Gershenson, V. N. Gubankov, and Yu. E. Zhuravlev, *Zh. Eksp. Teor. Fiz.* **85**, 287 (1983) [*Sov. Phys.—JETP* **58**, 167 (1983)].
- ⁴B. Shinozaki, T. Kawaguti, and Y. Fujimori, *J. Phys. Soc. Jpn.* **52**, 2297 (1983).
- ⁵G. Bergmann, *Phys. Rev. B* **29**, 6114 (1984).
- ⁶P. Santhanam and D. E. Prober, *Phys. Rev. B* **29**, 3733 (1984); P. Santhanam, S. Wind, and D. E. Prober, *ibid.* **35**, 3188 (1987).
- ⁷G. Bergmann, *Phys. Rep.* **107**, 1 (1984); P. A. Lee and T. V. Ramakrishnam, *Rev. Mod. Phys.* **57**, 287 (1985); S. Kobayashi and F. Komori, *Prog. Theor. Phys. Suppl.* **84**, 224 (1985); early related papers are summarized in their references.
- ⁸H. Fukuyama, *Physica* **126B**, 306 (1984); S. Maekawa, H. Ebisawa, and H. Fukuyama, *Prog. Theor. Phys. Suppl.* **84**, 154 (1985); related papers are summarized in their references.
- ⁹H. Raffy, R. B. Laibowitz, P. Chaudhari, and S. Maekawa, *Phys. Rev. B* **28**, 6607 (1983).
- ¹⁰J. M. Graybeal and M. R. Beasley, *Phys. Rev. B* **29**, 4167 (1984).
- ¹¹B. J. Dalrymple, S. A. Wolf, A. C. Ehrlich, and D. J. Gillespie, *Phys. Rev. B* **33**, 7514 (1986).
- ¹²M. Hikita, Y. Tajima, and T. Tamamura, in *Proceedings of the International Symposium on Anderson Location, Tokyo, 1987*, Vol. 28 of *Springer Proceeding in Physics*, edited by T. Ando and H. Fukuyama (Springer-Verlag, Berlin, 1988), p. 207.
- ¹³H. Ebisawa, S. Maekawa, and H. Fukuyama, *J. Phys. Soc. Jpn.* **55**, 4408 (1986).
- ¹⁴J. M. Graybeal, P. M. Mankiewich, R. C. Dynes, and M. R. Beasley, *Phys. Rev. Lett.* **59**, 2697 (1987).
- ¹⁵P. Santhanam, S. Wind, and D. E. Prober, *Phys. Rev. Lett.* **53**, 1179 (1984); S. Wind, M. J. Rooks, V. Chandrasekhar, and D. E. Prober, *ibid.* **57**, 633 (1986).
- ¹⁶S. Hikami, A. I. Larkin, and Y. Nagaoka, *Prog. Theor. Phys.* **63**, 707 (1980).
- ¹⁷C. Van Haesendonck, M. Gijs, and Y. Bruynseraede, in *Localization, Interaction and Transport Phenomena*, edited by B. Kramer, G. Bergmann, and Y. Bruynseraede (Springer-Verlag, Berlin, 1985), p. 221.
- ¹⁸A. I. Larkin, *Pis'ma Zh. Eksp. Teor. Fiz.* **31**, 239 (1980) [*JETP Lett.* **31**, 219 (1980)].
- ¹⁹E. Abrahams, R. E. Prange, and M. J. Stephan, *Physica* **55**, 230 (1971).
- ²⁰B. L. Alt'shuler, A. G. Aronov, and D. E. Khmel'nitsky, *J. Phys. C* **15**, 7367 (1982).
- ²¹E. Abrahams, P. W. Anderson, P. A. Lee, and T. V. Ramakrishnam, *Phys. Rev. B* **24**, 6783 (1981).
- ²²H. Fukuyama and E. Abrahams, *Phys. Rev. B* **27**, 5976 (1983).
- ²³H. Fukuyama, *J. Phys. Soc. Jpn.* **53**, 3299 (1984).
- ²⁴E. Abrahams, in *Localization, Interaction and Transport Phenomena*, edited by B. Kramer, G. Bergmann, and Y. Bruynseraede (Springer-Verlag, Berlin, 1985), p. 245.
- ²⁵W. E. Lawrence, and A. B. Meador, *Phys. Rev. B* **18**, 1154 (1978).
- ²⁶A. Schmid, in *Localization, Interaction and Transport Phenomena*, edited by B. Kramer, G. Bergmann, and Y. Bruynseraede (Springer-Verlag, Berlin, 1985), p. 212.
- ²⁷H. Takayama, *Z. Phys.* **263**, 329 (1973).
- ²⁸Yu. Kagan and A. P. Zhernov, *Zh. Eksp. Teor. Fiz.* **50**, 1107 (1966) [*Sov. Phys.—JETP* **23**, 737 (1966)].
- ²⁹H. Raffy, L. Dumoulin, P. Nedellec, and J. P. Burger, *J. Phys. F* **15**, L37 (1985).
- ³⁰H. Ebisawa, H. Fukuyama, and S. Maekawa, *J. Phys. Soc. Jpn.* **54**, 2257 (1985).
- ³¹S. I. Park and T. H. Geballe, *Physica* **135B**, 108 (1985).
- ³²M. Kakuchi, M. Hikita, and T. Tamamura, *Appl. Phys. Lett.* **48**, 835 (1986); M. Kakuchi, M. Hikita, A. Sugita, K. Onose, and T. Tamamura, *J. Electrochem. Soc.* **133**, 1755 (1986).
- ³³M. Grunder and J. Halbritter, *J. Appl. Phys.* **51**, 397 (1980).
- ³⁴G. Gladstone, M. A. Jensen, and J. R. Schrieffer, in *Superconductivity*, edited by R. D. Parks (Marcel Dekker, New York, 1969), Chap. 13, p. 174.
- ³⁵S. I. Park and T. H. Geballe, *Phys. Rev. Lett.* **57**, 901 (1986).
- ³⁶H. Fukuyama, in *Localization, Interaction and Transport Phenomena*, edited by B. Kramer, G. Bergmann, and Y. Bruynseraede (Springer-Verlag, Berlin, 1985), p. 51.
- ³⁷S. Maekawa and H. Fukuyama, *J. Phys. Soc. Jpn.* **52**, 1352 (1981); S. Maekawa and H. Fukuyama, *ibid.* **51**, 1380 (1982).
- ³⁸C. Camerlingo, P. Scardi, C. Tosello, and R. Vaglio, *Phys. Rev. B* **31**, 3121 (1985).
- ³⁹J. H. Quateman, *Phys. Rev. B* **34**, 1948 (1986).
- ⁴⁰S. Maekawa, H. Ebisawa, and H. Fukuyama, *J. Phys. Soc. Jpn.* **53**, 2681 (1984).
- ⁴¹A. G. Aronov, S. Hikami, and A. I. Larkin, *Phys. Rev. Lett.* **62**, 965 (1989).
- ⁴²Y. Matsuda, T. Hirari, S. Komiyama, T. Terashima, Y. Bando, K. Iijima, K. Yamamoto, and K. Hirata, *Phys. Rev. B* **40**, 5176 (1989).
- ⁴³M. Hikita and M. Suzuki, *Phys. Rev. B* **41**, 834 (1990).
- ⁴⁴H. R. Kerchner, D. K. Christen, and S. T. Sekula, *Phys. Rev. B* **24**, 1200 (1981).



1 µ m

FIG. 2. SEM photograph of Nb patterns with 1000-Å-width and 80-Å-thickness Nb pattern used for the measurement.